Analysis of the land cover change in large irrigated districts in the Yellow River basin using time series of Landsat and AVHRR

M. Matsuoka, Y. Fukushima and T. Hayasaka
Research Institute for Humanity and Nature
335 Takashima-cho Kamigyo-ku, Kyoto 602-0878, Japan
matsuoka@chikyu.ac.jp

Y. Honda
Center for Environmental Remote Sensing, Chiba University
1-33 Yoyoi-cho Inage-ku, Chiba 263-8522, Japan

T. Oki
Institute of Industrial Science, University of Tokyo
4-6-1 Komaba Meguro-ku, Tokyo 153-8505, Japan

Abstract: For the purpose to detect the change of agricultural area in large irrigation districts in the Yellow River basin, the method to estimate the agricultural area accurately using coarse resolution sensor i.e. AVHRR was developed on the Ningxia irrigation district. The agricultural area was calculated with higher spatial resolution sensor i.e. Landsat ETM+ by land cover classification, and it was correlated with annual maximum NDVI derived from AVHRR in order to get the fraction of agricultural area within one AVHRR pixel. The AVHRR estimation result showed the good agreement with ETM+ calculation in the county based comparison.
Keywords: Land cover change, Irrigation districts, Yellow River, Landsat, AVHRR.

1. Introduction

The Yellow River in China had been dried up and river water had not reached to the Bohai sea for many days in the year since 1970s. Therefore, the Yellow River Studies [1] is going on for the purpose to develop the hydrological model which helps the appropriate management of the water resource. Since one of the main reasons of the dry up is the increase of the agricultural water use in the large irrigation districts located in the upstream of the Yellow River, change detection of the agricultural area is essential for the model development. The purpose of this study is to detect the change of the agricultural area seamlessly for 20 years since early 80s using AVHRR (Advanced Very High Resolution Radiometer) data in the large irrigation districts in the Yellow River basin.

The outline of the study is shown in Fig. 1. The multi-temporal metrics such as annual maximum NDVI (Normalized Difference Vegetation Index) (Ann_Max_NDVI) derived from the time series of AVHRR are used to estimate the agricultural area for each year. Additionally, Landsat series are used in several points of time for the accurate calculation of agricultural area, since it has much higher spatial resolution and long heritage of operation. The Landsat result are used for the tuning and the validation of the estimation method by AVHRR.

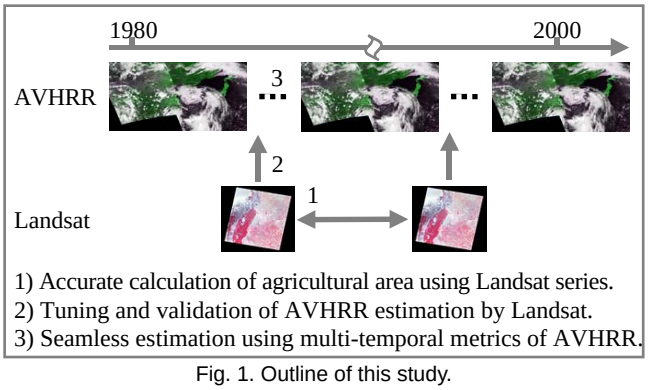

Fig. 1. Outline of this study.

In this paper, we describe the current status of this study. The method to estimate the fraction of agricultural area (Frac_Agri_Area) within one AVHRR pixel is developed based on the relation between Frac_Agri_Area and Ann_Max_NDVI in the Ningxia irrigated district for the year of 1999. This correspond to the part of 1 and 2 in Fig. 1.

2. Method and data

The method consists of following five procedures.

- Georectification of ETM+ to overlay to AVHRR.
- Land cover classification and calculation of agricultural area by ETM+.
- Production of daily AVHRR data set and derivation of Ann_Max_NDVI.
- Regression of Frac_Agri_Area and Ann_Max_NDVI.
- Estimation of the Frac_Agri_Area using AVHRR.

Two scenes of Landsat ETM+ (Path: 129, raw: 33 and 34) observed on August 12, 1999 were downloaded from Global Land Cover Facility [2] website and georectified to the equirectangular projection (so-called latitude/longitude projection). The coverage area is from 37 to 40 degrees north in latitude and from 105.5 to 107.5 degrees east in longitude. The spatial resolutions are 28.91 and 28.46 meters in north-south and east-west directions respectively. The top of atmosphere reflectance was calculated for each band, and NDVI was derived from reflectances in band 3 and 4.

The simple decision tree classification was applied to the ETM+. The classification flow is shown in Fig. 2. The single or multiple criteria were configured in each decision step to categorize the pixel to five kinds of land cover. GTOPO30 [3] was utilized as digital elevation model in decision 2. The threshold values were decided by the visual interpretation of the classification result.

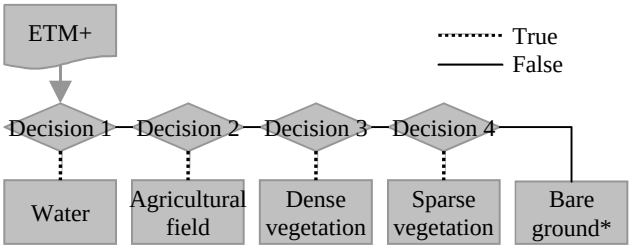

* Including built-up area

Decision	Criteria	Thresholds
1	NDVI < Threshold AND	0.400
	Ref5 < Threshold	3.75 %
2	Elevation < Threshold AND	1800 m
	NDVI > Threshold AND	0.350
	Ref5 < Threshold	25.0 %
3	NDVI > Threshold	0.375
4	NDVI > Threshold	0.250

Fig. 2. Flow of the decision tree classification.

Daily data of AVHRR in 1999 were produced with the spatial resolution of 30 arc seconds (approx. 928 meters at equator) from HRPT (High Resolution Picture Transmission) and LAC (Local Area Coverage). These source data were provided by Kitsuregawa Laboratory [4] in Univ. of Tokyo and Comprehensive Large Array-data Stewardship System [5] respectively. Since the geometric accuracy of AVHRR data is insufficient for our purpose, the precise geometric correction using GCP (ground control point) derived from MODIS (Moderate Resolution Imaging Spectroradiometer) was applied to each AVHRR path data. The example of the product on July 27, 1999 is shown in Fig. 3. After the elimination of poor corrected data and scan edge data, 169 data sets were used for this study.

The study area was clipped from all AVHRR data. Since the spatial resolution of AVHRR data is 30 arc seconds, 32 and 25 ETM+ pixel were correspond to one AVHRR pixel in north-south and east-west directions respectively. Ann_Max_NDVI was derived from this time series of AVHRR data. The maximum value was calculated by the averaging of five NDVI values from 2nd to 6th maximum in the year.

Frac_Agri_Area within the AVHRR pixel was calculated from classification of ETM+, and linear equation to estimate the Frac_Agri_Area from Ann_Max_NDVI was derived by the regression of these data.

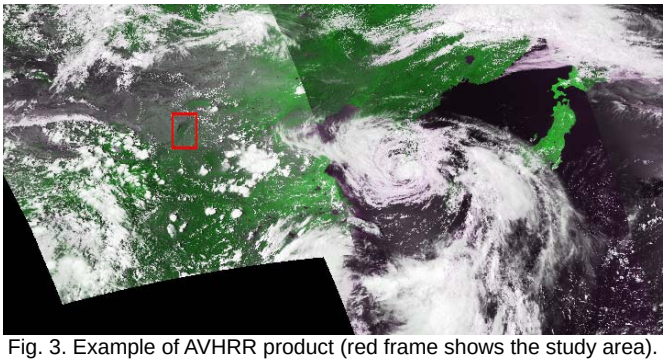

Fig. 3. Example of AVHRR product (red frame shows the study area).

The Frac_Agri_Area was estimated for whole area of Ningxia irrigation district by means of this regression equation. Because the dense vegetation category located on mountain has higher NDVI, these area (elevation > 1800 m) were masked by the GTOPO30 in order to avoid the miss-estimation of the Frac_Agri_Area. Furthermore, the lower NDVI region where the Ann_Max_NDVI is lower than 1.71 was regarded as non-agricultural region and eliminated from the estimation. The threshold value of 1.71 was derived by the averaging of Ann_Max_NDVI pixels which the fraction of sparse vegetation is over 90 %.

3. Results and discussions

The land cover classification map derived from ETM+ is shown in Fig. 4 (a). Fig. 4 (b) shows the county based comparison of agricultural areas against census in 1999 recorded in the Statistical Yearbook of Ningxia [6]. Although the comparison of land cover classification with registration based census is not straightforward generally as described by Frolking et al. [7] and Hansen et al. [8] the result shows the good agreement except Yanchi county where most of the agricultural area is non-irrigated, and therefore, was classified as sparse vegetation.

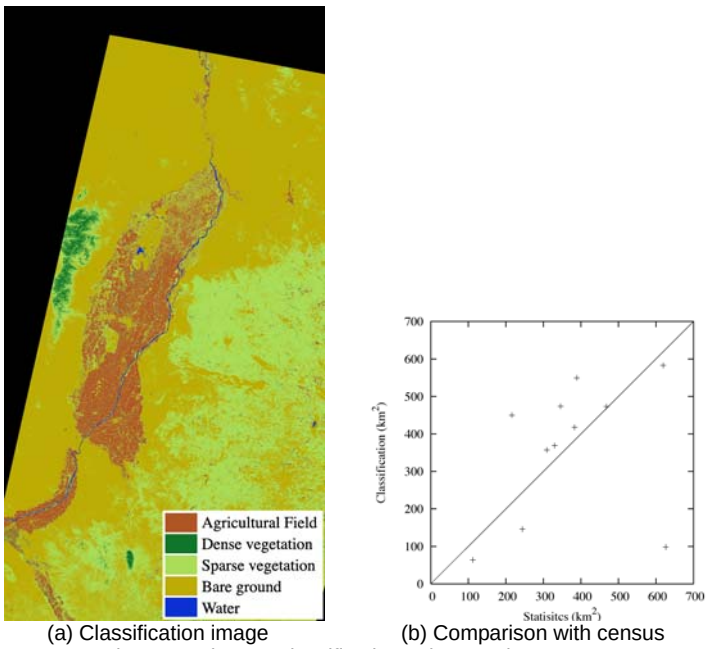

(a) Classification image (b) Comparison with census

Fig. 4. Land cover classification using Landsat ETM+.

Fig. 5 (a) is the Ann_Max_NDVI derived AVHRR and Fig. 5 (b) is the scattergram of Frac_Agri_Area against the Ann_Max_NDVI. Ann_Max_NDVI shows the higher contrast of the irrigated districts with other natural land This contrast i.e. higher NDVI in irrigated field and lower NDVI in arid region, enables us to associate Ann_Max_NDVI directly with Frac_Agri_Area. The scattergram shows clear linear relation between them though the dispersion is large. Eq. (1) is the linear equation derived from the regression.

$$Frac\_Agri\_Area = 2.54 \times Ann\_Max\_NDVI - 0.330 \quad (1)$$

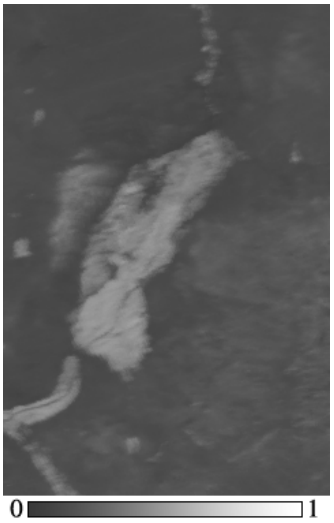

(a) Ann_Max_NDVI image (b) Scattergram of Ann_Max_NDVI and Frac_Agri_Area

Fig. 5. Ann_Max_NDVI and its relation to Frac_Agri_Area.

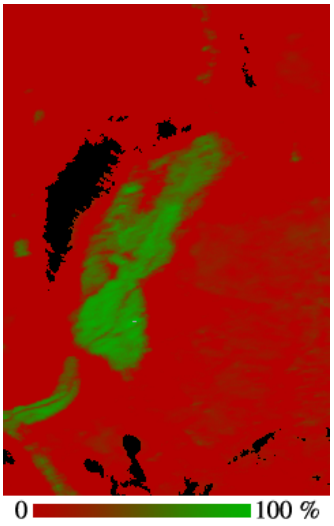

(a) Fraction of agricultural area (b) Comparison with ETM+ result

Fig. 6. Estimation of the fraction of agricultural area by AVHRR.

Fig. 6 (a) shows the Frac_Agri_Area estimated from AVHRR data set, black area is the mountainous area masked by GTOPO30 described above. Fig. 6 (b) shows the county based comparison of agricultural areas derived from ETM+ and AVHRR. Agricultural area estimated from low resolution AVHRR data shows the almost same value with high resolution calculation by ETM+ in county basis.

4. Conclusions

Simple method to estimate the fraction of agricultural area within the AVHRR pixel was developed for the purpose to detect the change of agricultural area accurately in the large irrigation district in the Yellow River basin. This method is based on the assumption that higher NDVI is corresponds to the irrigated agricultural area, therefore the method is specialized for the irrigated districts in the arid region. The method will be validated by means of another periods of AVHRR and Landsat data, and thereafter it will be applied to the time series of AVHRR data for 20 years.

Acknowledgement

This study has been carried out as a part of the Research Revolution 2002 project supported by the Ministry of Education, Culture, Sports, Science and Technology (MEXT) in Japan.

Authors appreciate the valuable distribution of HRPT by Kitsuregawa Lab., LAC data by Comprehensive Large Array-data Stewardship System, Landsat by Global Land Cover Facility, and GTOPO30 by USGS.

References

[1] The Yellow River Studies. (2003). http://www.chikyu.ac.jp/yris/.
[2] Global Land Cover Facility. (1997). http://glcf.umiacs.umd.edu/index.shtml.
[3] GTOPO30 - Global Topographic Data. (2004). http://edcdaac.usgs.gov:80/gtopo30/gtopo30.asp.
[4] Kitsuregawa Laboratory. (2005). http://www.tkl.iis.u-tokyo.ac.jp/english/.
[5] Comprehensive Large Array-data Stewardship System. (2005). http://www.class.noaa.gov/nsaa/products/welcome.
[6] Statistical Yearbook of Ningxia. (2000).
[7] Frolking, S., Xiao, X., Zhuang, Y., Salas, W., and Li, C. (1999). Agricultural land-use in China: a comparison of area estimates from ground-based census and satellite-borne remote sensing. Global Ecology and Biogeography, 8: 407-416.
[8] Hansen, M. C., Defries, R. S., Townshend, J. R. G., and Sohlberg, R. (2000). Global land cover classification at 1 km spatial resolution using a classification tree approach. Int. J. Remote Sensing, 21(6): 1331-1364.